EMSP Annual and Final Report, June 2005

Investigating Ultrasonic Diffraction Grating Spectroscopy and Reflection Techniques for Characterizing Slurry Properties

DE-FG07-01ER63297 Project Number: 81889

Lead Principal Investigator:
Margaret S. Greenwood
Pacific Northwest National Laboratory
Richland, WA 99352
509-375-6801
margaret.greenwood@pnl.gov

Co-Investigator:
Leonard J. Bond
Pacific Northwest National Laboratory
Richland, WA 99352
509-375-4486
leonard.bond@pnl.gov

Co-Investigator:
Lloyd Burgess
University of Washington
Seattle, WA 98195
206-543-0579
lloyd@cpac.washington.edu

Co-Investigator:
Anatol Brodsky
University of Washington
Seattle, WA 98195
206-543-1676
brodsky@cpac.washington.edu

Graduate Student:
Mazen Lee Hamad
University of Washington
Seattle, WA 98195
mhamad@u.washington.edu

Research Objectives

The size of particles in a slurry and the viscosity of a liquid or slurry are difficult to measure both on-line and in real time. The objectives of this research are to develop the following methods for such measurements: 1) Ultrasonic Diffraction Grating Spectroscopy (UDGS) to measure the particle size of a slurry, 2) UDGS to measure the velocity of sound in

a slurry using reflection from a grating as opposed to ultrasound traveling through a possibly dense slurry, and 3) shear wave reflection techniques to measure the viscosity of a slurry. UDGS is an analytical technique that is the ultrasonic analog of an optical technique called Grating Light Reflection Spectroscopy (GLRS). GLRS was pioneered at the University of Washington, with ongoing research in this area and two issued U.S. patents, 5,610,708 and 5, 502,560.

The UDGS research efforts have been performed as a collaborative effort between the Pacific Northwest National Laboratory (PNNL) and the University of Washington (UW). The principle investigator (PI) on the project was Margaret S. Greenwood at PNNL, and the co-PI's were Leonard J. Bond at PNNL, and Lloyd W. Burgess and Anatol M. Brodsky at the UW. A 3 year award was granted from the U.S. Department of Energy Environmental Management Science Program (DOE-EMSP) for the proposal entitled, "Investigating Ultrasonic Diffraction Grating Spectroscopy and Reflection Techniques for Characterizing Slurry Properties", February 2001, under contract DE-AC06-76RL01830. The purpose of this project was to give the researchers the opportunity to develop the ultrasonic equivalent of GLRS for applications in dense slurries. In general, the experimental portion of the research was carried out at PNNL, and the UW researchers provided insights into the theoretical aspects of the project as well as with data analysis. **A two year renewal has been granted to the experimental group at PNNL and a no cost extension to the UW group to permit the completion of analysis of preliminary data and this report. This report contains the final UW work on this project.**

Introduction

The goal of the UDGS project was to build a non-invasive sensor capable of measuring characteristics of slurries in steel pipelines. This type of sensor would be especially useful for monitoring the flowing contents of steel pipes connected to radioactive waste storage tanks at the U.S. Department of Energy Hanford Site,[1] as well as in many other process monitoring and control applications.

The UDGS sensor developed under these efforts resembles the on-line ultrasonic density sensor, which was developed by Greenwood and co-workers[2] at PNNL. A schematic of the on-line ultrasonic density sensor is shown in figure 1. The on-line ultrasonic density sensor consists of six ultrasonic transducers mounted onto a Rexolite™ wedge, which is placed in contact with a liquid sample. The six send and receive transducers are mounted on the Rexolite™ wedge at different angles with respect to the normal of the Rexolite™-liquid interface. The purpose of the send and receive transducers was to measure the reflection coefficients from the Rexolite™-sample interface at two different angles. Then, the density of the liquid sample and the speed of sound in the sample could be determined from the reflection coefficients. Therefore, the on-line ultrasonic density sensor actually measured the speed of sound and the density of the sample. A practical aspect of this sensor was that it could be used to measure samples in pipelines (by mounting the sensor onto a pipe), or it could be used to measure samples in a tank (by submerging the sensor into the tank).

---

[1] Details about the nuclear waste clean up efforts at Hanford can be found at www.hanford.gov.

[2] Greenwood, M. S.; Skorpik, J. R.; Bamberger, J. A.; Harris, R. V. *Ultrasonics,* **1999**, *37*, 159-171.

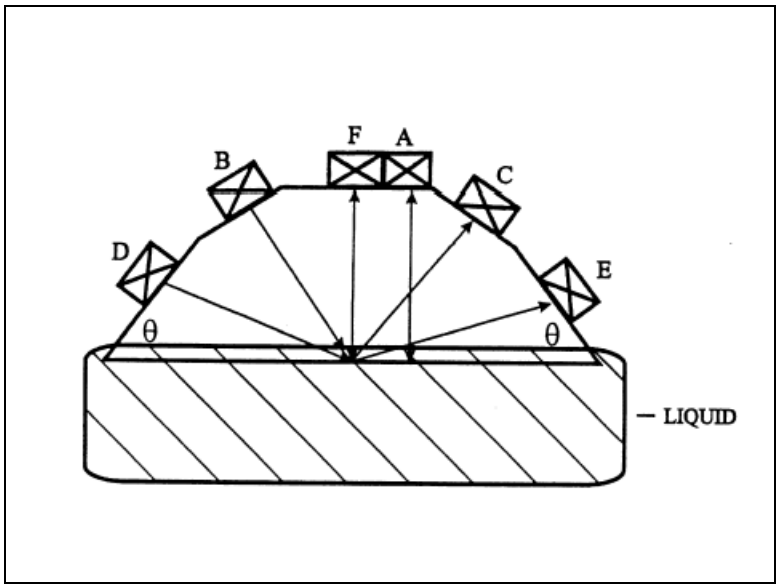

Figure 1. On-line ultrasonic density sensor consists of six send and receive transducers mounted onto a Rexolite™ wedge. This figure was taken from Greenwood, et al.[2]

The UDGS sensor was built in a similar manner to the on-line ultrasonic density sensor. A 3-dimensional representation of the UDGS sensor is shown in figure 2. The body of the UDGS sensor was made of stainless steel, as opposed to the Rexolite™ used in the on-line ultrasonic density sensor. The respective materials were chosen because UDGS yields a higher signal to noise ratio with a larger reflection from the grating-sample interface, whereas the on-line ultrasonic density sensor yields a higher signal to noise ratio with a smaller reflection from the grating-sample interface. And it turns out that a stainless steel-water interface has a large impedance mismatch, which yields a large reflection; whereas the Rexolite™-water interface has a small impedance mismatch, which yields a smaller reflection.

The UDGS gratings can be produced using standard machining equipment. To build the UDGS sensor, a short section of stainless steel rod was cut in half, and two flats were cut at a 30^{o} angle with respect to the normal. A send transducer was mounted on one of the flats, and a receive transducer was mounted on the other flat. A 300 micron grating with a 120^{o} included angle triangular groove profile was machined into the bottom side of the sensor. In contrast to the straight forward construction of the UDGS sensor, the equipment required to construct the gratings for GLRS was very specialized.

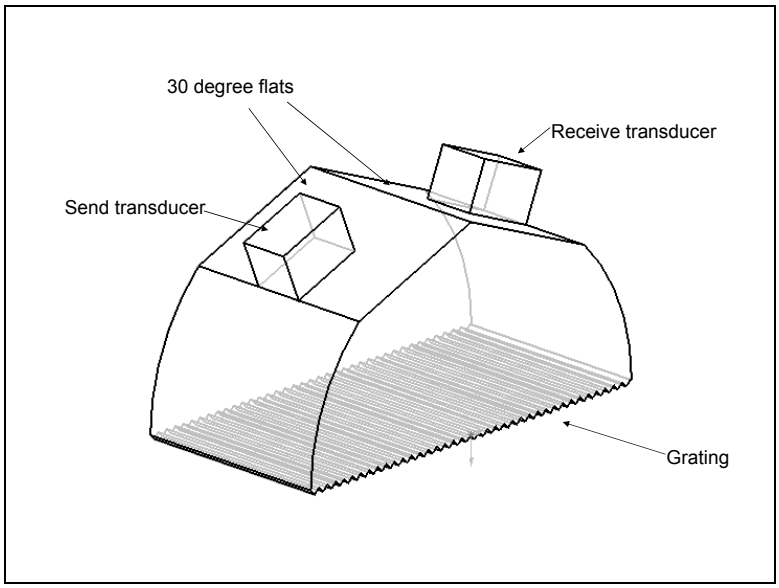

Figure 2. Schematic of the UDGS sensor.

To operate the sensor, the grating of the UDGS sensor was placed in contact with a liquid sample and the send transducer was used to send a toneburst of a specific frequency toward the grating-sample interface. Then, the reflected signal from the grating-sample interface was collected with the receive transducer. After the signal was received, the frequency of the toneburst was increased by a small amount and another signal was sent and collected. This process was repeated until the desired frequency range was covered. The frequency range could be from as low as 2 MHz to as high as 10 MHz, and the typical step size was 0.05 MHz. The collected data yielded a plot of reflected intensity as a function of frequency, and this reflectance spectrum contained singularities with frequencies and intensities that depended on the ultrasonic properties of the sample. This is analogous to the optical case (GLRS) where the reflected spectrum contains singularities that depend on the optical properties of the sample.

Some of the fundamental differences between UDGS and GLRS should be considered along with their respective analytical implications. For certain applications, such as slurry characterization in pipelines, the acoustic version of GLRS will have several advantages over conventional GLRS. For example, the penetration depth of the evanescent field will change dramatically between the ultrasonic and the optical case. The evanescent field penetration depth is proportional to the critical wavelength, therefore, the increase in the penetration depth from the GLRS case to the UDGS case will be a factor of approximately 600, as determined by considering a 500 nm critical wavelength in GLRS compared with a 5 MHz (yielding a wavelength of 300 μm in water) critical frequency in UDGS. This increase in penetration depth over the GLRS case is expected to give the UDGS sensor greater ability to detect the bulk contents of the sample in the pipeline.

The differences in wavelengths of the incident waves between the optical and ultrasonic cases will cause the two techniques to respond differently to particles of different sizes. The wavelengths for ultrasonic waves traveling in water in the 4 to 12 MHz range will be from 120 to 370 microns. The optical wavelengths in water for UV, visible, and near-IR light will range from 150 nm to 1300 nm, or 0.15 microns to 1.3 microns. The upper limit of

applicability of the Rayleigh scattering regime is reached when the wavelength of the penetrating radiation becomes comparable with the particle dimension. The scattering amplitude increases monotonically up to this limit, after which it oscillates in characteristic resonance behavior.[3]

In general, the above-mentioned theories indicate that GLRS will be most sensitive to particles in the sub-micron diameter range, whereas UDGS will be more sensitive to particles that are several hundred microns in diameter. This clarifies that GLRS and UDGS actually provide complementary information about the sample's mean particle size.

The specifics of propagation of ultrasonic waves and light waves should be considered. Light waves are electromagnetic transverse waves with two polarization states: the p-polarized state and the s-polarized state. Ultrasonic waves are pressure waves, which can be shear waves or longitudinal waves. The shear waves are transverse waves with two polarization states: the shear horizontal and the shear vertical, corresponding to s-polarized and p-polarized optical waves, respectively. The ultrasonic longitudinal waves have no optical analogy.

As mentioned previously, the goal of the UDGS sensor project is to measure the characteristics of slurries in pipelines. The sought after characteristics of the slurries include speed of sound, viscosity, mean particle size, and particle size distribution. All of these characteristics of the slurry have important consequences with respect to their influence on the transport properties of the slurry. For example, an increase in viscosity may provide insight into the possibility of slurry vitrification in the pipeline, or an increase in the mean particle size may indicate a potential clog inside the pipeline.

Theoretical Considerations of UDGS

In the following, we consider the scattering of longitudinal waves. The diffraction grating equation, also called the Bragg equation, is used to derive the optical critical frequencies found in GLRS.[4,5] A similar derivation can be to show that the ultrasonic critical or singular frequencies found in UDGS are:

$$\omega_{cr} = \frac{2\pi m c_i}{\Lambda\left(\frac{Sin\,\theta_i}{c_i} + \frac{1}{c_d}\right)}, \qquad [1]$$

where ω_{cr} is the critical frequency, m is the diffracted order, c_i is the velocity of the incident waves, Λ is the period of the diffraction grating, θ_i is the angle of incidence, and c_d is the velocity of the diffracted waves. Equation 1 is used to calculate the expected critical frequencies for a given set of experimental conditions and will be used in the results and discussion sections to compare the experimental critical frequencies to the expected critical frequencies.

The theory describing the expected reflectance from the grating-sample interface has been developed by Anatol Brodsky at UW. The equation for the theoretical ultrasonic

---

[3] Van de Hulst, H.C. *Light Scattering by Small Particles*, Dover Publications, pp. 75, 174-179.
[4] Palmer, C. Diffraction Grating Handbook. 4th ed.; Richardson Grating Laboratory: New York, 2000.
[5] Hutley, M. C. Diffraction Gratings. Academic Press Inc.: New York and London, 1982.

reflectance spectrum from a grating-sample interface takes on the same general form as the equation for the theoretical light reflectance spectrum from a grating-sample interface. The equation for the theoretical ultrasonic reflectance spectrum is written as follows

$$I = A_0 + A_1\sqrt{\sqrt{\delta^2+\kappa^2}+\delta} + A_2\sqrt{\sqrt{\delta^2+\kappa^2}-\delta}\,, \qquad [2]$$

where I is the reflected intensity from the grating-sample interface, and A_0, A_1, and A_2 are coefficients that depend on the properties of the grating, the properties of the sample, and the frequency of ultrasonic waves. These coefficients remained approximately constant in the "threshold interval" of frequencies.

$$\left|\frac{\omega-\omega_{cr}}{\omega_{cr}}\right| < 1\,, \qquad [3]$$

The term κ in equation 2 is the attenuation term, which is analogous to the imaginary part of the complex dielectric function in optics. The term κ is defined as

$$\kappa = \frac{2\omega^3\gamma}{3c^4}\,, \qquad [4]$$

where γ is the kinematic viscosity of the sample and c is the speed of sound in the sample. The kinematic viscosity, often measured in Stokes (cm^2/s), is the absolute, or dynamic, viscosity of a substance divided by its density (mass/volume). Equation 2 states that measurement of the attenuation term (κ) with the UDGS sensor allows the kinematic viscosity (γ) to be determined. The kinematic viscosity (γ) is a sample property that is directly related to the flow properties of a sample.

In figure 3, a plot of equation 2 shows that the theoretical reflectance spectrum contains a single peak. The frequency of the peak depends on the speed of sound in the sample and the height of the peak depends on the attenuation in the sample. The first derivative of the reflected intensity with respect to the angular frequency ($dI/d\omega$) is plotted in figure 4. The first derivative plot has two peaks, a maximum peak and a minimum peak. The first derivative plot in figure 4 shows very sharp peaks; this is the case when the kinematic viscosity is small. As the kinematic viscosity increases, the first derivative peaks become smaller and wider. The case representing a large kinematic viscosity is shown in figure 5. These theoretical predictions are of great value because they can be compared with experimental observations to help with the data analysis.

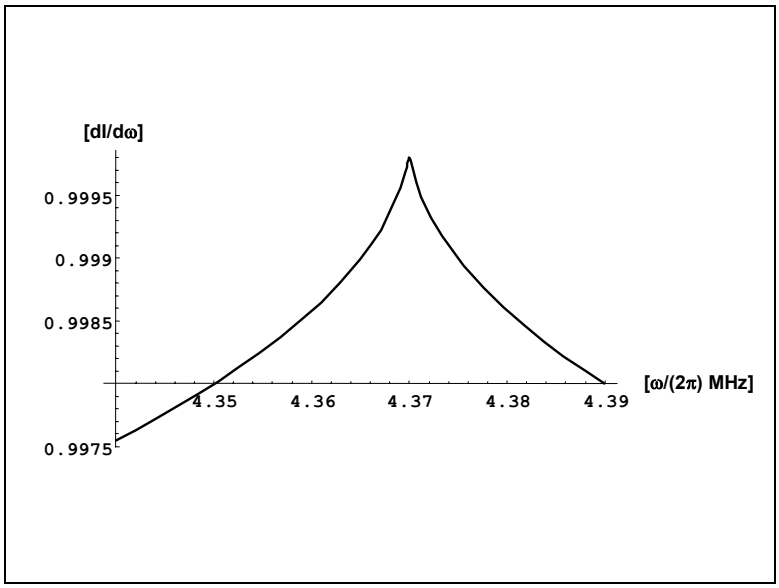

Figure 3. The UDGS theoretical reflectance spectra for the case when the kinematic viscosity (γ) is close to zero.

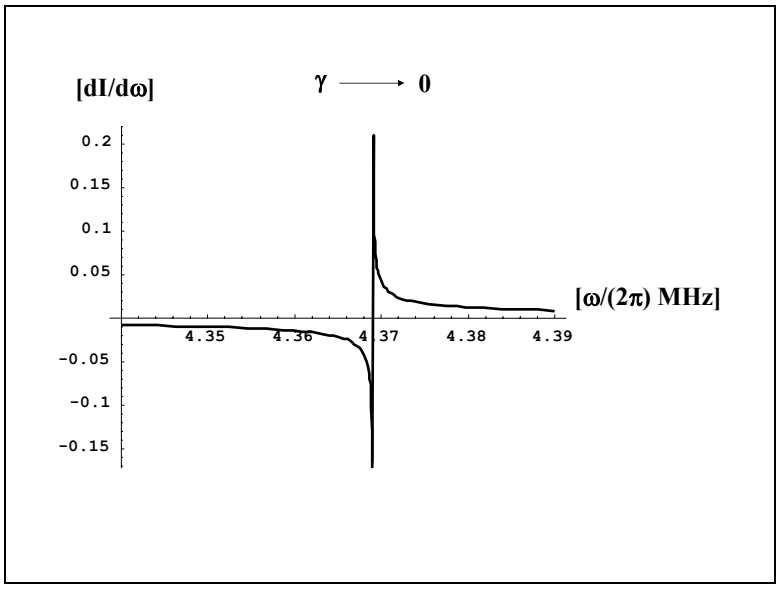

Figure 4. The UDGS theoretical first derivative of reflectance plot for the case when the kinematic viscosity (γ) is close to zero.

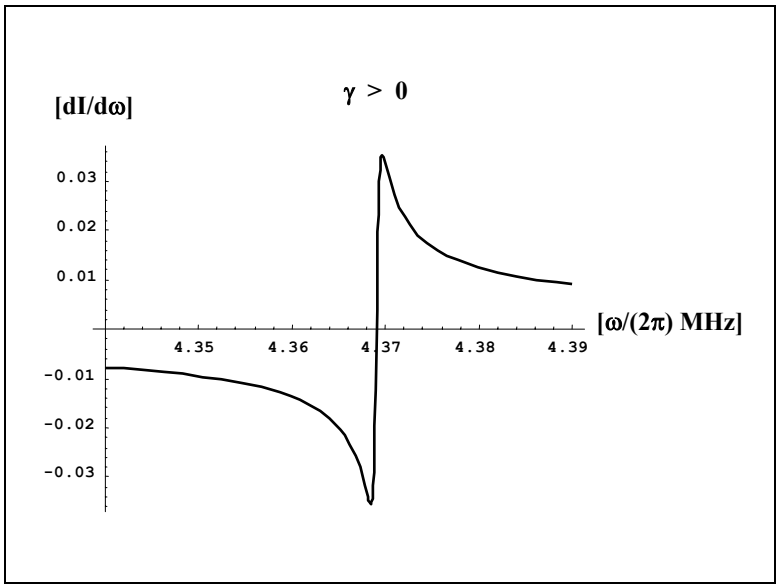

Figure 5. The UDGS theoretical first derivative of reflectance plot for the case when the kinematic viscosity (γ) is close to zero. The differences between figure 4 and 5 show that the peak height, peak width, and peak position depend on the kinematic viscosity (γ).

Analysis of Solutions of Sugar in Water

The data presented in this section was collected at PNNL by Margaret S. Greenwood and coworkers, using the UDGS sensor represented in figure 2. The angle of incidence for this experiment was 30 degrees, and the period of the stainless steel grating was 300 microns. A longitudinal toneburst was sent by the send transducer, and the reflected ultrasound was collected with the receive transducer. The frequency was scanned from 3.5 MHz to 7.5 MHz, in 0.05 MHz steps. Data was collected for a series of aqueous sugar samples with concentrations of 0, 10, 15, 20, 25, and 30 (w/w)% sugar. A reference spectrum was collected for each sample. The reference spectrum was obtained by collecting data for each sample with a reference sensor. The reference sensor was similar to the UDGS sensor; however it did not contain a grating. The sample contacting surface of the reference sensor was a flat plane. Each sample spectrum was divided by the reference spectrum to eliminate the response functions of the send and receive transducers.

Two UDGS water spectra are plotted in figure 6. These water spectra provide an example of the appearance of the experimentally determined reflectance spectra. The spectra have peaks at approximately 5.5 MHz and the calculated critical frequency for water is 5.67 MHz, a bias of only 0.12 MHz. This shift can easily be explained by the fact that the angle of incidence is only accurate to about 0.5 degrees. The signal, estimated as the height of the peaks, is approximately 3 times the peak to peak noise of the spectra. The peak to peak noise is approximately 5 times the standard deviation of the signal; therefore these spectra have a relatively low signal to noise ratio of approximately 15.

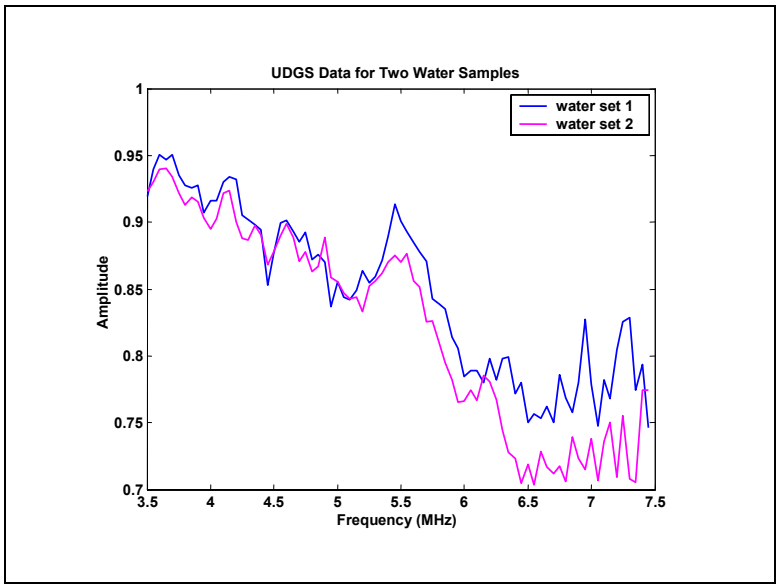

Figure 6. UDGS data collected for two water samples.

The first derivatives of the spectra were taken to help facilitate the data analysis. A Savitsky-Golay algorithm was used to find the derivatives of the spectra.[6] The Savitsky-Golay algorithm is built into the PLS toolbox (Eigenvector, Manson, WA), which is a supplement to the Matlab program (The Mathworks, Inc., Natick, MA). A 3rd order polynomial, 13 point wide Savitky-Golay first derivative filter was used to process each of sugar solution spectra. The results are given in Figure 7.

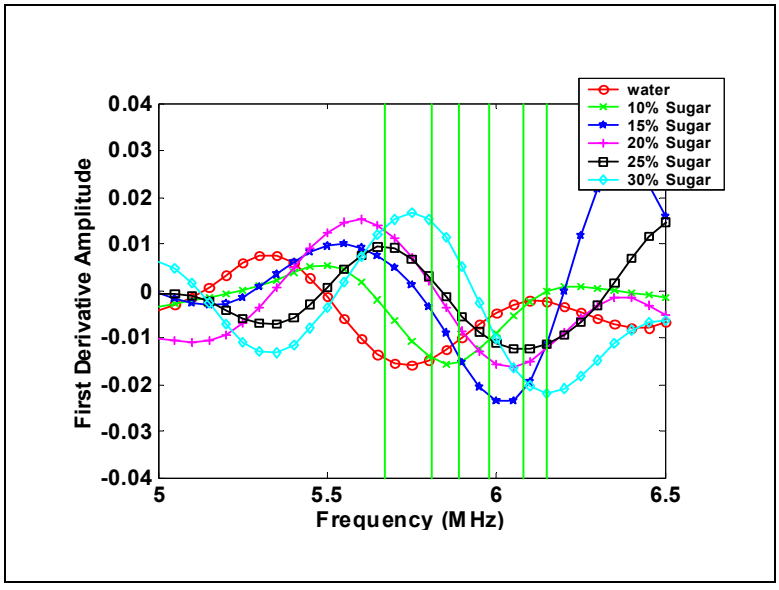

Figure 7. UDGS first derivative plot for 6 sugar water solutions. The vertical lines represent the calculated critical frequencies for the sugar water solutions (water is at the lowest frequency and 30% sugar is at the highest frequency).

[6] Savitsky, A.; Golay, M. J. E. *Analytical Chemistry*. **1964**, *36,* 1627-1639.

The next step in analyzing the data was to fit a spline interpolant to the first derivative spectra. As shown in figure 8 for a water sample, the spline interpolant is used to increase the data density of the first derivative spectra. The original first derivative spectrum has data points at an interval of every 0.05 MHz, and the spline interpolant has data points at an interval of every of 0.005 MHz. Thus, the data density has increased by a factor of 10. The increase in data density allows the peak maxima and peak minima to be determined more accurately.

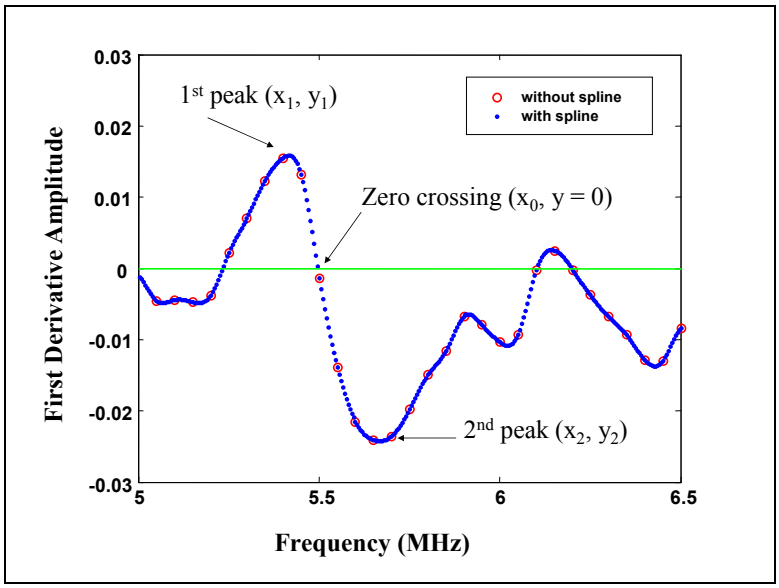

Figure 8. A spline interpolant fit to a UDGS first derivative plot for water. A 13 point, third order polynomial, first derivative Savitsky-Golay filter was applied to the reflectance data prior to fitting with the spline interpolant.

There are five data points of interest that are taken from the spline interpolated first derivative plots: the x and y positions of the peak maximum (x_1, y_1), the x and y positions of the peak minimum (x_2, y_2), and the x position of the zero crossing. The maximum peak frequency, the zero crossing frequency, and the minimum peak frequency for all sugar solutions are shown in figure 9, plotted against their respective sugar concentrations. This plot shows that there is an increase in the position of the peak frequency as the sugar concentration is increased. Thus, there are three different data points that can be used to measure the sugar concentration. The positions of all of these data points shift with sugar concentration because the velocity of sound is a function of sugar concentration.

It is predicted that the change in viscosity associated with a change in sugar concentration will cause a change in the peak heights of the first derivative spectra. As the concentration of sugar increases, the viscosity of the solution increases; and an increase in viscosity is expected to cause the peak heights to decrease. Further work needs to focus on measuring changes in peak heights as a function of viscosity.

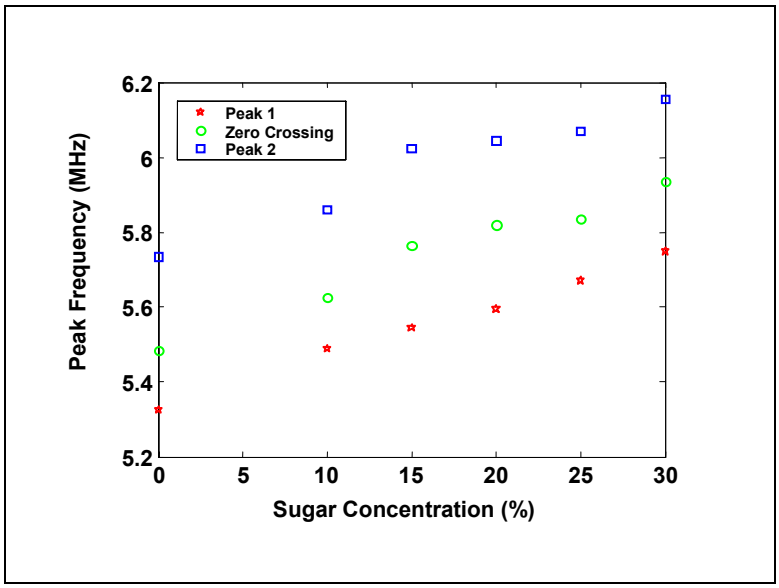

Figure 9. Peak frequency vs. sugar concentration for 0.05 MHz step data.

Analysis of Polystyrene Microspheres in Water

During the last year of this project, the main objective of the theoretical work at the University of Washington has been to develop a method to calculate the ultrasonic dissipation parameters from the experimental data with slurries. The theory of ultrasonic wave back scattering by a slurry at the boundary of a diffraction grating interface has been developed. Much information can be obtained near the critical frequency where the traveling waves are transformed into evanescent ones. Analysis of ultrasonic scattering in this region allows us to get rich information about both the surface and bulk properties of the sample. There are two mechanisms that occur when the evanescent wave interacts with particles in the slurry. One mechanism is coherence loss in the scattering process. The second one takes into account the wave absorption, which is dependent upon the kinematic viscosity. For small particles, wave absorption prevails, where $R\,(\nu/\omega)^{0.5} < 1$. R is the particle radius, ν is the kinematic viscosity and ω is the angular frequency. For large particles, where $R(\nu/\omega)^{0.5} > 1$, the dissipation mechanism is dominated by incoherent scattering effects. The dissipation function $\varepsilon(R)$ can be found by analysis of the signal near the critical frequency. In particular, the peak height of the derivative of the signal at the critical frequency is inversely proportional to $[\varepsilon(R)]^{0.5}$.

To evaluate the effect of the particle size on the UDGS response, experimental measurements were obtained for nominally monodispersed polystyrene spheres with diameters of 16, 42, 74, 98, and 136 microns, each at 10% by weight with 1-4 replicates at each particle size. The experimental measurements were made with the stainless steel grating (240 microns) with transducers epoxied to the stainless steel unit. For measurements with slurries, a semi-circular cup having a radius of 0.75 inches was attached to the front of the stainless steel grating unit.

The UDGS raw data and the effect of smoothing the data with a 9 point, 3rd order polynomial Savitzky-Golay filter are shown in Fig. 10. The smoothing filter provides a good

approximation to the raw signal, while eliminating much of the high frequency, point-to-point perturbations.

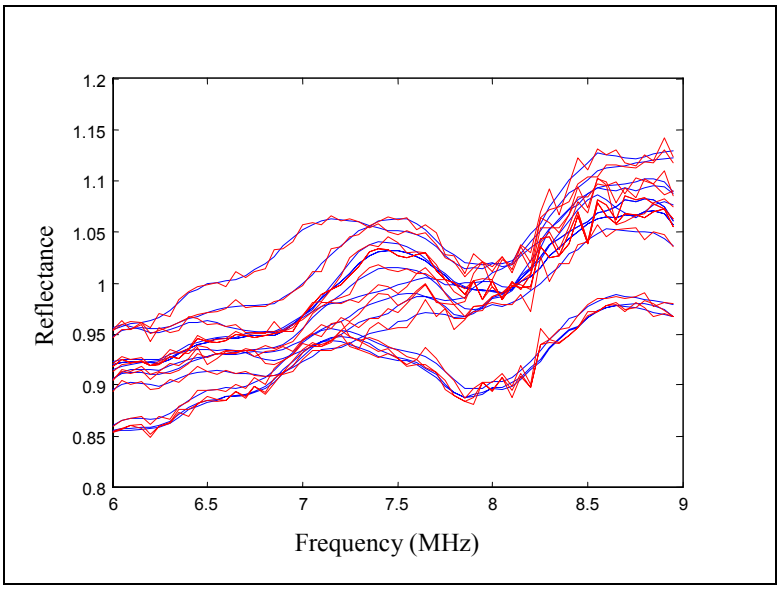

Figure 10. Polystyrene sphere data, raw and with the application of a Savitzky-Golay smoothing filter. This simply illustrates that the smoothed data (blue) represents the raw signal well.

The first derivative of the data in figure 10 was evaluated and is shown in figure 11. Several effects are noticeable in the first derivative plot, including a shift in the peak frequency for the 74 micron particle curves and shift in the peak height between the smaller particles (16 and 42 micron) and the larger particles (98 and 136 micron).

Further classification analysis was performed with a Principal Components Analysis (PCA), which reduces intensities on the spectral axis into scores on a small number of principal components (PCs). In a PCA scores plot, proximity of the samples provides an indication of sample similarity. After processing the raw signal into the first derivatives, a PCA was performed and the resulting 3-dimensionsal PCA scores plot is shown in figure 12. The PCA scores plot shows that each particle size and its replicates form clusters within this space, meaning that each set has yielded a unique UDGS signal. This implies particle sizing with UDGS is certainly possible utilizing a fairly simple model.

The theoretical aspects of the UDGS response to heterogeneous slurries have been further developed. The theory states that, under the given conditions (ie; polystyrene in water), the ultrasonic response function (ε) will drop to a minimum for particles with diameters near 50μm. Our observations support the prediction of UGDS resonance behavior, and opens an important perspective for its application in slurry characterization.

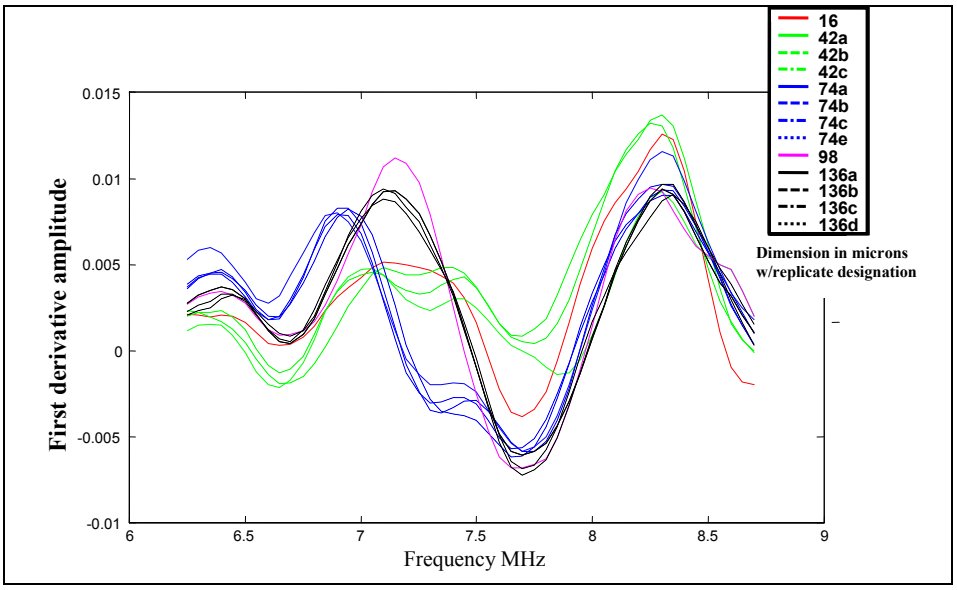

Figure 11. 15 point SG derivative applied to Figure 10. Data consists of from 1 to 4 replicates at each particle size as noted in sidebar.

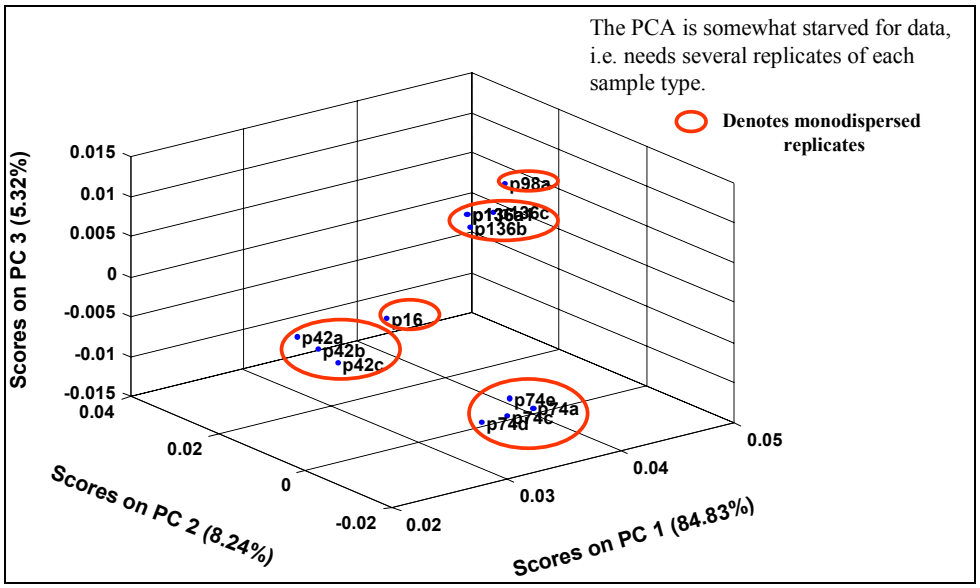

Figure 12. 3-dimensional PCA scores plot of 1st derivative data, illustrating the clustering of the response at each particle size.

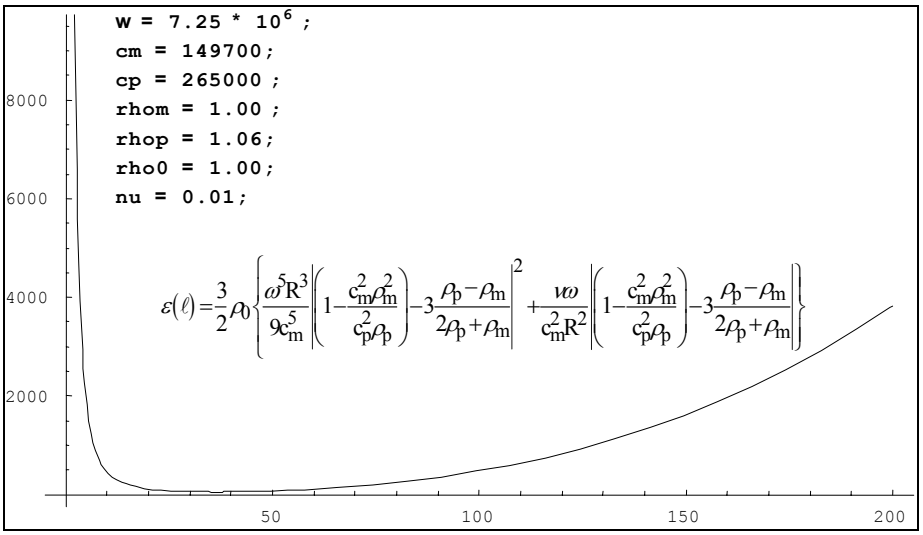

Figure 13. ε plotted as particle size changes, showing transition around 50 microns consistent w/data

Conclusion

These experiments provide evidence that significant progress toward the construction of a useful UDGS sensor has been achieved. Several UDGS sensor prototypes have been constructed and these new devices are capable of measuring the velocity of sound in a sample as well as providing sensitivity to heterogeneous mixtures containing different particle sizes. The benefits of this sensor are that it functions as a reflectance sensor, and thus only has to make contact with a liquid sample at a single interface in order to operate.

The success of the UDGS project has been achieved despite there being only a limited amount of information available about acoustic or ultrasonic diffraction gratings. Very few references of ultrasonic gratings that diffract ultrasonic waves exist in the literature, and therefore, this research has provided evidence that the ultrasonic gratings function in a similar manner to optical gratings. With this work as a basis, it may be found that ultrasonic gratings will have many other uses besides their use as UDGS sensors, just as optical gratings have many other uses besides their use as GLRS sensors.

It is expected that this sensor will be capable of making accurate viscosity and particle sizing measurements in the near future. But before these measurements can be made, improvements in the sensor design must be made to boost the signal to noise ratio of the measurement. Experiments have already been performed that show that the UDGS singularity shape can be improved by increasing the number of grating slits illuminated by the ultrasound.[7] Further improvement in the signal to noise ratio is expected to be achieved when the p-polarized shear component is collected and used in the PCA model. During these experiments, only the longitudinal components were collected. It is clear that there is not a large effect in the longitudinal beam, but it is expected that the shear components will give rise to much larger signal changes.

[7] Greenwood, M. S.; Brodsky, A. M.; Burgess, L. W.; Bond, L. J.; Hamad, M. L. *Ultrasonics.* 42, 531-536 (2004).